Accepted Manuscript

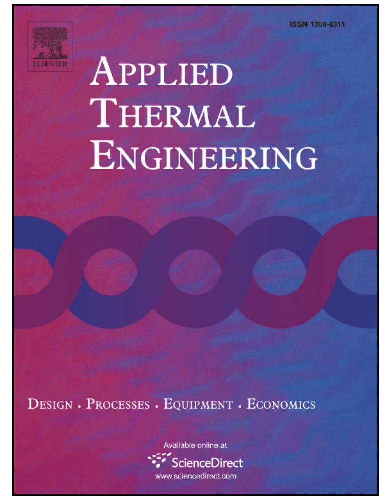

Research Paper

A study on exergetic performance of using porous media in the salt gradient solar pond

Hua Wang, Qi Wu, Yanyang Mei, Liugang Zhang, Shusheng Pang

PII: S1359-4311(17)37663-9
DOI: https://doi.org/10.1016/j.applthermaleng.2018.03.025
Reference: ATE 11913

To appear in: *Applied Thermal Engineering*

Received Date: 1 December 2017
Revised Date: 26 January 2018
Accepted Date: 6 March 2018

Please cite this article as: H. Wang, Q. Wu, Y. Mei, L. Zhang, S. Pang, A study on exergetic performance of using porous media in the salt gradient solar pond, *Applied Thermal Engineering* (2018), doi: https://doi.org/10.1016/j.applthermaleng.2018.03.025

A study on exergetic performance of using porous media in the salt gradient solar pond

Hua Wang[1], Qi Wu[1], Yanyang Mei[1,*], Liugang Zhang[1] Shusheng Pang[2]

1. *School of Mechanical and Power Engineering, Henan Polytechnic University, 2001 Century Avenue, Jiaozuo 454003, Henan, P. R. China*
2. *Department of Chemical and Process Engineering, University of Canterbury, Christchurch, 8025, New Zealand*

Abstract: The transient exergetic performance of the salt gradient solar ponds with porous media added in Lower Convective Zone (LCZ) is investigated. One dimensional transient temperature, energy and exergy models have been developed. Three different porous media materials have been used in the simulation. Findings show that solar pond with cinders gains the highest LCZ temperature and gets the maximum energy and exergy efficiency which are 32.62 % and 20.70 % respectively, and the lowest one is the case with marbles which are 29.72% and 16.62%. The results indicate that adding porous media with low volume heat capacity and low heat diffusivity to LCZ is beneficial to reach a higher temperature, and high temperature, high volume heat capacity and low thermal diffusivity of the porous media are both positive effect to the solar pond's energy and exergy storage. Experimental study shows that the numerical energy and exergetic efficiency are both a little higher than experimental ones, and the same temperature difference leads to a bigger exergy difference than energy.

Key words: solar pond; porous media; exergy; energy; simulation

1. Introduction

China government has set the target of increasing the share of renewable energy

[*] Corresponding author.
E-mail address: 1987myy525@163.com

consumption to 15% by 2020 [1]. Due to the high solar energy and rich salt resources potential in China, thermal applications based on salt gradient solar ponds are interesting options for the future energy demand. However, solar pond only provides heat lower than 100 ℃[2], energy and exergy performance is particularly important for such low heat source application.

Researchers have tried to improve the energy efficiency of the solar ponds [3-6].An approach is to integrate solar pond with collector system, and this has been studied to increase solar pond performance by Bozkurt and Karakilcik [7]. A.A. Abdullah et al. shared the experience of constructing a 113 m^2 solar pond, and a new approach for the purpose of enhancing performance which is sustainable heat extraction system from solar pond has been presented [8]. A. Alcaraz et al. (2016) investigated the effect of enhancing the efficiency of solar pond by extracting heat from both lateral and bottom, and found that heat extracted from the lateral improves the efficiency of solar pond [1]. To increase the entire system's efficiency, there are also some experimental and theoretical studies were investigated about integrated solar pond with different applications [9-15].

For heat storage equipment, it is important not only to collect or store a certain quantity of energy but also to do so at the highest possible temperature [16]. The quality of heat energy which can be express by the exergy of unit mass is depended on the heat source temperature. Though there is report states that in some cases pool temperatures as high as 110 °C in an outdoor solar pond [17], in fact, under normal operation condition, solar pond is not easy to reach a higher temperature than 80 ^{o}C [1, 12].

It is obvious that increasing solar pond temperature is a directly way to increase the exergy of unit mass of solar pond. Researchers have found that adding some porous media materials in LCZ can increase solar pond temperature. In 1998, Al-Juwayhel and El-Refaee [18] numerically presented that adding porous media in LCZ could increase the LCZ temperature. Wang et.al [19, 20] has studied the influence porous media on the temperature of LCZ. Some researchers investigated the influence of porous media on solar pond stability or the behavior of salt diffusion [21-23]. A.A. Hill and M. Carr found that solar ponds that contain porous media are more stable than the solar ponds without adding any porous media [21].

To evaluate the exergy performance of solar ponds is of essence, since the purpose of a heat storage system is not only to store energy, but also to store exergy, which is the quantity of real value [24, 25], Some researchers investigated the energy and exergy performance of a traditional solar pond which without any porous media [7, 10, 26, 27, 28]. However, to the best of our knowledge, there is no research report about the exergy performance of solar pond with porous media.

Above all, the exiting research reports have proved introducing some porous media to LCZ of solar pond is benefit to improve the temperature of solar ponds; and in order to evaluate the effectiveness, it is necessary to investigate the exergy performance of the solar pond with porous media in LCZ.

The objective of this work is to investigate the effect of adding porous media in LCZ on the transient exergetic performance of solar pond. The paper firstly presents the numerical model for the temperature prediction and energy and exergy analysis; and secondly, the transient energy and exergy results for adding three porous media and traditional solar pond (without any porous media) cases are compared and discussed. In addition, an experimental study used to compare to the numerical modeling.

2. Modeling

To analysis the energy and exergy behavior of the solar pond, the temperature distribution and evolution is the fundamental step. In this study, An one dimensional problem for the large solar pond is considered, which means, temperature only changed in depth direction, and the temperature horizontally difference is ignored, and a solar pond with so large surface that the heat loss from the lateral wall is ignored. Though wall shading has a great effect on small solar pond [29], it can be neglected for large area solar pond in this study. The coastal city Tian Jin (39º 50′ N), China is chosen as the place where the solar pond operates. As shown in Fig.1, the depth of the modeling solar pond is 2 m. UCZ, NCZ and LCZ are 0.20 m, 1.0 m and 0.8 m respectively. The inner zone of the model solar pond is divided into 40 (which is I presented in Fig.1) imaginary layers with a thickness of Δx=0.05 m; the time step is one hour, Δt=3600s.

Boundary and initial conditions are given as following.

- Surface water temperature equals to ambient temperature, and the bottom of the solar pond is assumed to be insulated with 0.50 m thickness of glass-wool, which is a feasible insulating type and also used in Ismail Bozkurt et al.'s research [7].
- For the salinity distribution, assume the UCZ is filled with freshwater; the density range of NCZ is 1010 to 1190 kg/m^3 which increase downward by increment of 10 kg/0.05m; and the LCZ is filled with concentrated brine water with density of 1200 kg/m^3.

- The initial temperature of the whole solar pond is assumed as the local ambient temperature.
- The modeling solar pond was operated from April 10, and the temperature evolutions during 2 years have been simulated.
- Heat extraction from solar pond is taken as the 10% of the total energy storage.
- In addition, solar pond thermal performance is significantly affected by the losses of heat through bottom, soil below the bottom of solar pond act as a heat sink of solar pond [30]. In this study, ground temperature is considered as a constant of local mean annual temperature.

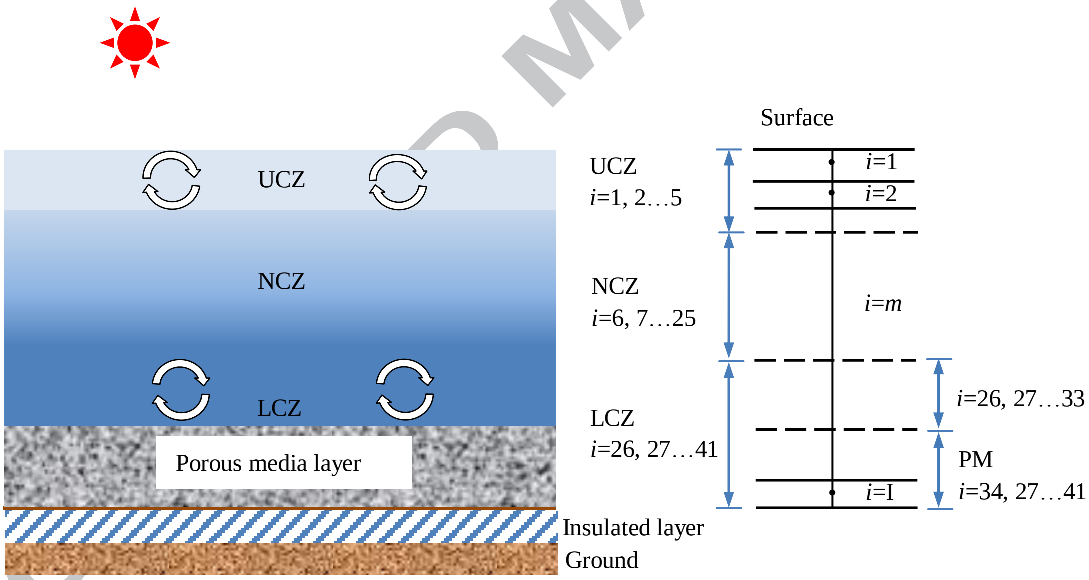

Fig. 1 schematic and the One-dimensional discretization of solar pond with porous media

2.1 Equations

The problem under study is considered as a transient behavior of the one dimensional heat transfer inside the solar pond.

$$\frac{\partial T}{\partial t} = k\frac{\partial^2 T}{\partial x^2} + \frac{\dot{q}(x)}{\rho c_p} \tag{1}$$

where $\dot{q}(x)$ the rate of the energy generation per unit volume in the layer of depth of x, W/m^3; and it is related to extinction coefficient μ, m^{-1}. $\dot{q}(x)$ is expressed by[31, 32]

$$\dot{q}(x) = 0.6q(n, t)\mu \exp(-\mu x) \tag{2}$$

where $q(n,t)$ in Eq.(2) is the solar radiation incident on the water free surface, W/m^2, and can be expressed as follows [33]

$$q(n, t) = \frac{24 \times 3.6G_{sc}}{\pi}[1 + 0.033\cos(\frac{2\pi n}{365})]$$
$$\times \left(\cos\varphi\cos\delta\sin\omega_s + \omega_s\sin\varphi\sin\delta\right) \times \left[a + b\frac{n_i}{N}\right] \tag{3}$$

where G_{sc} is the solar constant, and G_{sc} =1353 W/m^2, and a and b is the correction factor related to the local climate，in this study, a and b is 0.248, 0.752 respectively[33], n_{i} /N is called percentage of sunshine, that is the ratio of the actual and astronomical hours of sunshine, which n_{i} can be got from the local climate data, N is calculated by the following equation

$$N = \frac{2}{15} \times \frac{180\cos\left(-\tan\delta\tan\varphi\right)}{\pi} \tag{4}$$

where φ is latitude, rad; δ is the declination angle of the sun, rad; and ω is the time angle, rad; the equations of them as following,

$$\delta = \frac{23.45\pi}{180}\sin(\frac{360(284 + n)}{365.25}) \tag{5}$$

$$\omega = \frac{2\pi(t-12)}{24} \tag{6}$$

where n is the day number during a year which counted from January 1, and t is the time which expressed by 24 h a day.

The detail discrete equations for every zone of solar pond can be obtained according to the above equations, and the expressions of the variables (δ and ω) in Eq. (4) can be found from literature [19].

The temperature of the water surface layer is assumed as atmosphere temperature T_0, and it can be calculated by the following empirical formula [33]

$$T_0(t) = \overline{T} + 0.489\Delta T \cos\frac{\pi(t - 15.05)}{12} \tag{7}$$

where $\overline{T}$ (ºC) is the monthly mean daily temperature, which can be get from the local weather service; and ΔT (ºC) is the daily temperature range.

For LCZ, consider that heat extraction as a part of heat storage, assume f is the fraction of the heat flux extracted to the total heat flux absorbed, then $\dot{q}(x)$ in LCZ can be expressed as following

$$\dot{q}(x) = (1 - f)0.6q(n, t)\mu \exp(-\mu x) \tag{8}$$

In the mixture zone of brine water and porous media, the thermal properties are depended on both of the mixtures, where ρ_m, C_m and k_m are density, thermal capacity and conductivity of the working mediums in the mixed zone of porous media layer respectively, and they are calculated by relating the properties of water (subscript 'w') and porous media (subscript 'pm') and the fractions as following:

$$\rho_m = \varepsilon \times \rho_i + (1 - \varepsilon) \times \rho_p \tag{9}$$

$$C_m = \varepsilon \times \frac{\rho_i}{\rho_m} \times C(c, T) + (1 - \varepsilon) \times \frac{\rho_p}{\rho_m} \times C_p \tag{10}$$

$$k_m = \varepsilon \times k_w + (1 - \varepsilon) \times k_p \tag{11}$$

In consideration of the convection occurs in top zone of LCZ, water conductivity k_w (W/mK) is assumed as 5 times of the conductivity of brine water which is expressed by following equation of Eq.(13).

2.2 Properties of brine water

In this study, heat capacity, C (kJ/kgK) of brine water is considered as the function of salinity c(kg/m^3); take density ρ (kg/m^3) and the thermal conductivity k (W/mK) as functions of c and T [34, 35]. The relationships of them are expressed by Eq. (12)- Eq. (14).

$$C = \left(4180 - 4.396c + 0.0048c^2\right) / 1000 \tag{12}$$

$$k(c, T) = 3.6 \times \left[0.5553 - 8.13 \times 10^{-4} c + 8 \times 10^{-4}(T - 293)\right] \tag{13}$$

$$\rho = 998 + 0.65c - 0.4(T - 20) \tag{14}$$

According to Eqs (2)-(14), discretized Eq.(1) with the finite volume discretization method, then the one-dimensional transient temperature field of solar pond can be get.

2.3 Energy analysis

Due to the low temperature and the difficulty in heat extraction, the energy stored in UCZ is ignored. The daily stored energy ΔE_{n} (MJ/m^2) in solar pond and heat extraction is calculated by

$$\Delta E_n = \sum_{i=7}^{I} \rho c \Delta x(\overline{T}_{n,i} - \overline{T}_{n-1,i}) + q_{\mathrm{ext},n} \tag{15}$$

where $q_{\mathrm{ext},n}$ represents the total heat extraction from solar pond on the nth day, MJ/m^2. According to the assumption of the modeling, it can be expressed by:

$$q_{ext,n} = 0.1 \times \Delta E_{n-1} \tag{16}$$

Then, the energy efficiency of the solar pond is expressed by

$$\eta_{en,n} = \frac{\Delta E_n}{E_{solar,n}} \tag{17}$$

where $E_{solar,n}$ is the daily total solar radiation energy incident in solar pond, MJ/m^2, where the sunshine hours is the from sunrise t_{s} to sunset t_{d}.

$$E_{solar,n} = \sum_{t=t_s}^{t_d} q(n,t) \tag{18}$$

2.4 Exergy analysis

In this study, exergy is evaluated from two sides, one is the daily exergy stored by solar pond for unit solar radiation area, ΔEx_n (MJ/m^2), and the other is the exergy the solar pond possesses, Ex_n (MJ/m^2), and since the heat extracted is the energy supplied by solar pond to applications, both of ΔEx_n and Ex_n includes the heat extraction item ($q_{\mathrm{ext},n}$).

2.4.1 Daily exergy increment ΔEx_n

The exergy stored by solar pond on the *n*th day can be expressed by,

$$\Delta Ex_n = \sum_{i=7}^{I}\left[\rho c\Delta x\left(\overline{T}_{i,n} - \overline{T}_{i,n-1}\right) - T_0\rho c\Delta x \ln\left(\frac{\overline{T}_{i,n}}{\overline{T}_{i,n-1}}\right) + q_{ext,i,n}\left(1 - \frac{T_0}{\overline{T}_{i,n}}\right)\right] \tag{19}$$

where $\overline{T}_{i,n}$ is the mean temperature of the *i*th layer on the *n*th day, K; $\overline{T}_{i,n\text{-}1}$ is the mean temperature of the *i*th layer on the (*n*-1)th day, K; take the reference temperature T_0 as the mean ambient temperature of the *n*th day, K.

The solar exergy Ex_{solar} (MJ/m^2) provided by Petela (2003) is utilized for evaluating the solar exergy at the surface of horizontal ground surface which is [36]:

$$Ex_{\mathrm{solar}} = E_{\mathrm{solar},n}\left[1 - \frac{4}{3}\frac{T_0}{T_{\mathrm{solar}}} + \frac{1}{3}\left(\frac{T_0}{T_{\mathrm{solar}}}\right)^4\right] \tag{20}$$

where $E_{\mathrm{solar},n}$ is expressed in Eq.(18); T_0 is the reference temperature and is calculated by Eq.(7); T_{solar} is sun's surface temperature which assumed to be 5770 K.

The exergy efficiency for solar pond may be defined as:

$$\eta_{ex,n} = \frac{\Delta Ex_n}{Ex_{\mathrm{solar},n}} \tag{21}$$

2.4.2 Daily exergy Ex_n

Besides of the above daily increasing solar energy, working as solar energy stored equipment, the exergy stored ability is also an important property to estimate its thermal performance. The following equation is used to estimate the exergy state of the *n*th day.

$$Ex_n = \sum_{i=7}^{I}\left[\rho c\left(\overline{T}_{i,n} - \overline{T}_{i,n-1}\right) - T_0\rho c \ln\left(\frac{\overline{T}_{i,n}}{T_0}\right) + q_{\text{ext},i,\ n}\left(1 - \frac{T_0}{\overline{T}_{i,n}}\right)\right] \tag{22}$$

3. Results and discussions

In order to study the effect of porous media on the energy and exergy performance of solar pond, four cases are considered in this study, which are case A, the traditional solar pond (without any porous media added); Case B, case C and case D are the same solar pond added different porous media with half thickness LCZ, which are marbles, limestones and cinders, respectively, and the porosities of them are all taken as 50%. Table 1 gives the main physical properties of the working mediums. The Density, heat capacity conductivity data of the porous media in Table 1 are got from measuring. Heat capacity is measured by Synchronous thermal analyzer STA 449F3 of NETZSCH, and conductivity is measured by a conductometer based on hot wire method. Thermal diffusivity is calculated based on the equation of $\alpha=k/(\rho c)$.

It can be found that brine water owns a maximum volume heat capacity and the minimum thermal diffusivity, however, due to the convection occurred in LCZ, the thermal diffusivity of brine water in Table 1 is only suitable for NCZ (where there is no convection occurs) and it has no meaning for LCZ. Among all of the materials, the thermal diffusivity of cinders is the smallest one.

Table 1 the main physical properties of the LCZ working mediums using in this study (at 50 °C)

Thermal properties	Brine	Marbles	Limestone	Cinders
Density/ ρ, kg/m^3	1200	2800	2400	1580
Heat capacity/ c, kJ/kg K	3.28	0.92	0.91	0.72
Conductivity/k, W/m K	0.58	2.90	2.04	1.03
volume heat capacity /ρc, kJ/m^3	3936	2576	2179	1136
Thermal diffusivity/α, m^2/s	1.47×10^{-7}	1.12×10^{-6}	9.36×10^{-7}	9.06×10^{-7}

In this section, the temperature evolution for the four cases for 2 years is presented, and according to the temperature results, energy and exergy efficiencies for the four cases are calculated. Though, the stability of the solar pond is important for long-term operation, salinity of NCZ is assumed constant considering the big salinity difference in NCZ of this study.

3.1 Temperature development

Fig. 2 depicts the temperature evolutions at different depths for the four cases, and also ambient temperature and solar radiation evolutions. Fig.3 gives the Daily mean LCZ temperature for four cases. As seen in Fig.3, the temperature increases towards the bottom of the solar pond, and reaches a maximum value around August, and then the temperature starts to decrease. The mean LCZ temperature are 51.59 ºC, 52.90 ℃, 55.20 ℃ and 60.78 ℃ for case A, case B, case C and case D during the two years. It is observed from Fig. 2 and Fig. 3, the maximum LCZ Temperature increases with the decreasing of the volume heat capacity (ρc) of the porous media. Take the second year as an example, case D is observed to be the maximum mean LCZ temperature of 92.8 ℃ on July 31, and 84.4 ℃ on Aug. 5 for case C, and 80.9 ℃ on Aug. 7 for case B, and 79.4 ℃ Aug. 7 for case A. Similarly, the lowest temperature decreases with the increasing of the volume heat capacity (ρc) of the porous media. The date on which solar pond reaches the maximum or the minimum temperature both delay with the increasing of the volume heat capacity (ρc) of the working medium of LCZ.

From Fig. 2, for the three cases with porous media, it is observed that the highest temperature all appears near the top interface of the mixed porous media zone. This can be understood that the opaque and dark color of the porous media results in the totally absorption of solar radiation that reaches on them. It is easy to deduce that the smaller the porosity of the porous media zone is the more solar irradiation absorbed by the top interface of the mixed porous media zone.

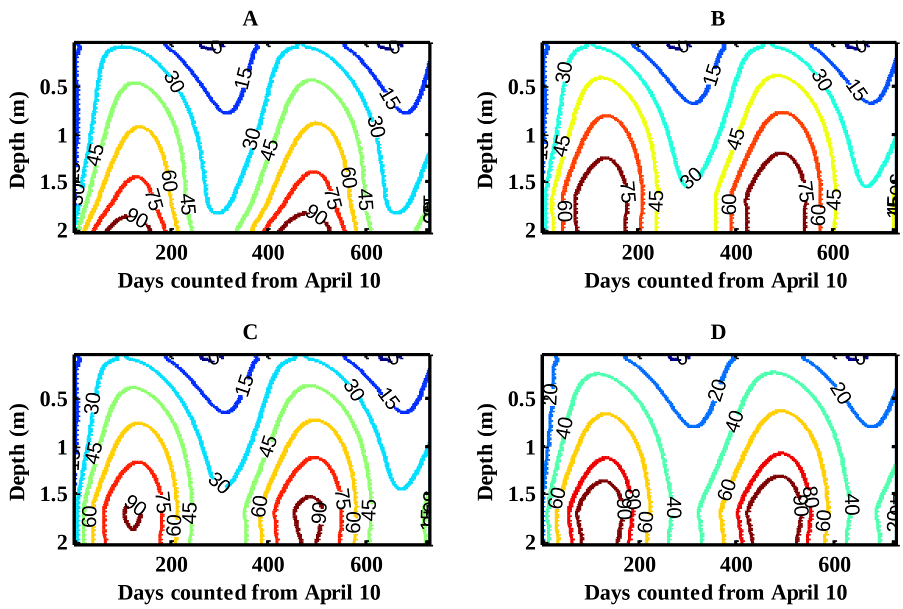

Fig. 2 Temperature evolutions during 2 years for four cases

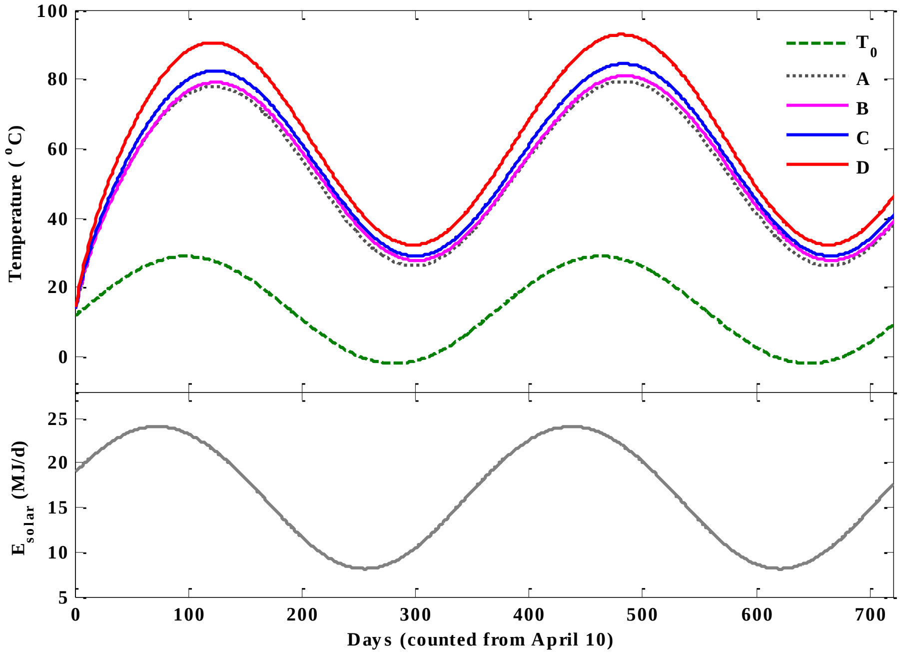

Fig.3 Daily average LCZ temperature for four cases, Daily ambient temperature and solar radiation (E_{solar})

3.2 Exergy evolution

Fig. 4 shows the daily exergy increments during two years which is calculated according to the expression in the Brace of Eq. (19). It is observed that the exergy increments of the first year are bigger than that of the second year; which is related to the temperature evolution. Take the second year as an example, for all of the four cases, exergy increases from early February to mid-August, which is caused by the variation of solar radiation and atmosphere temperature. For case A, daily exergy increment of each layer ($\Delta Ex_{i,n}$) reach the maximum value of 0.0251 MJ/m^2 on the 52th day; and which is 0.0178 MJ/m^2 on the 55th day for case B, 0.0197 MJ/m^2 on the 53th day for case C, 0.0260 MJ/m^2 on the 44th day for case D. The position where temperature reaches the maximum is in the bottom layer of the solar pond for case A; and which is around the depth of 1.70 m, 1.65 m and 1.65m for case B, C and D respectively. It also can be found in case D that the maximum exergy increment appears on the top interface of the porous media zone, which can be ascribed to the small thermal conductivity of the cinders. This suggests that the top part of LCZ with higher exergy increment should be the optimal heat extraction position.

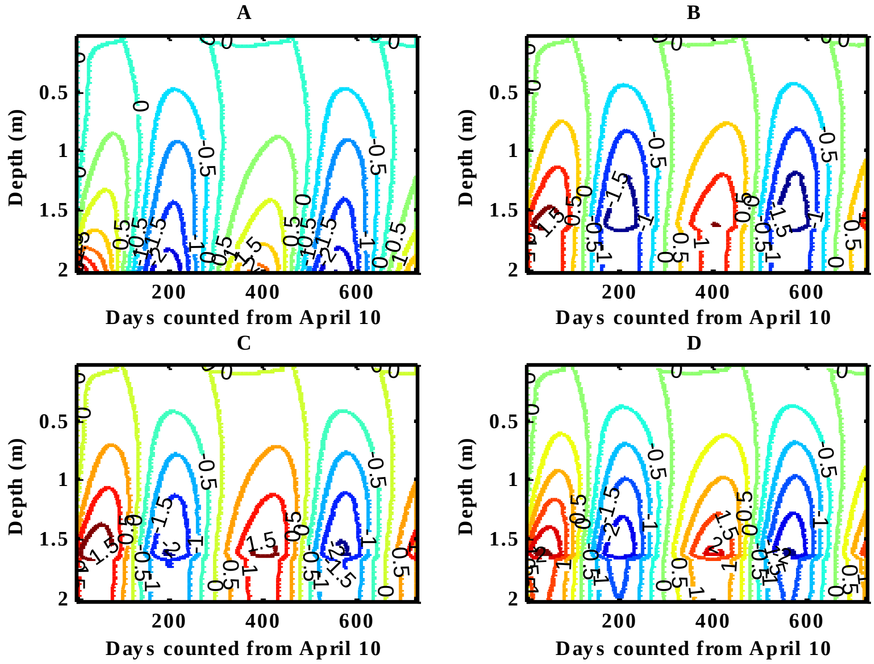

Fig.4 Daily exergy increment ($\Delta Ex_{i,n}$) contours for each calculated step (Δx=0.05 m) during 2 years for each case (MJ/m^2)

The exergy of the working mediums possess is also an important property for solar pond application, and it relates to the total amount of exergy storage. Fig. 5 shows the amount of the exergy $Ex_{i,n}$, and which is calculated by Eq.(22). Take the second year as example, the days the total exergy reaches the maximum are 506th (August 25), 534th (September 22), 521th (September 15) and 519th (September 13) day, and the amounts are 34.3, 27.10, 29.49 and 35.44 MJ/m^2 for the case A, B, C and D respectively. Associate with Table 1, it can be concluded that lower thermal diffusivity (α), higher temperature and volume result in a higher exergy.

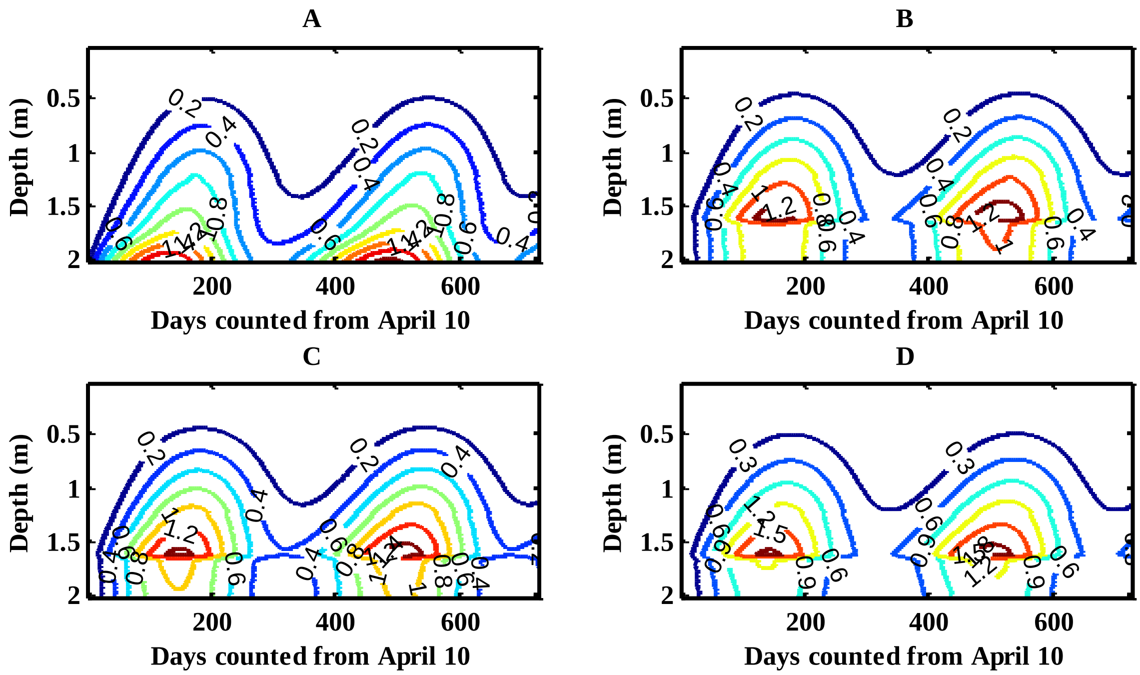

Fig.5 Daily exergy contours for each calculated step (Δx=0.05 m) during 2 years for each case (MJ/m^3)

3.3 Energy and exergy efficiencies

Fig.6 shows a comparison of both energy and exergy efficiencies. It is observed that the energy efficiency for the four cases are all increasing rapidly at the initial period, this is because that the solar radiation is much stronger and the initial temperature is very low. The energy efficiencies of the four cases are all around 30%, and case D has higher energy efficiency than the other three cases.

Different from energy efficiency, the evolutions of the exergy efficiencies for the four cases are all lower. The average exergy efficiencies are 20.08%, 16.62%, 17.77% and 20.70% for case A, B, C and D respectively. Case D has the highest exergy efficiency, case A is the second, and the lowest is case B. The results of energy and exergy efficiencies obtained in this study are similar to the corresponding values reported by Karakilcik and Dincer (2008) for experimental solar ponds (31° 36′ N) with insulated wall and bottom and with area and depth of 3 m^2 and 1.5 m, respectively [28].

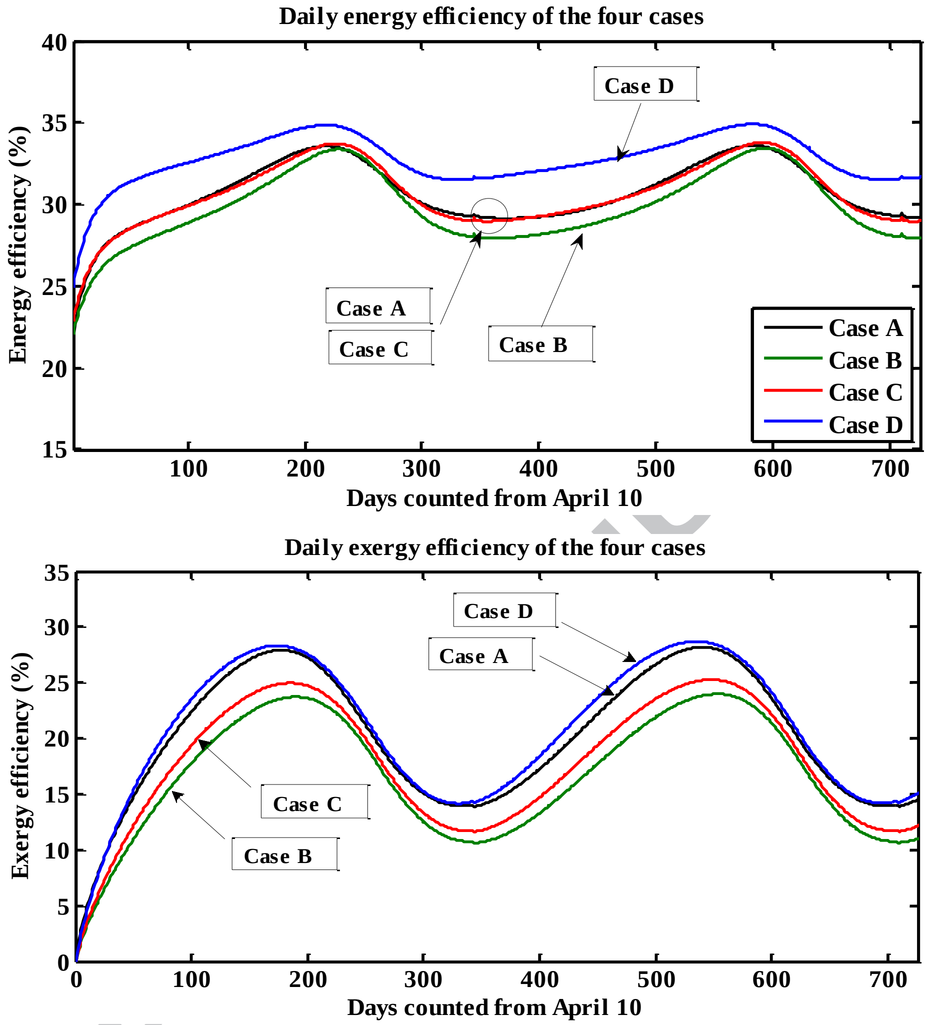

Fig.6 Daily energy efficiency (η_{en}) and exergy (η_{ex}) for the four cases

A comparison between energy efficiency and exergy efficiency shows that the order is different in the four cases. For the energy efficiency curves, the order of the maximum peak from big to small is case D, case C, case A and case B; and for curves of exergy efficiency the order of case B, case C and case D is same to the energy efficiency, only that case A has a greater improvement and which is almost up to case D. This is because that brine water has bigger volume capacity than that of cinders. The results of Fig.6 also indicates that proper heat extraction improves energy/exergy efficiency.

3.4 Experimental results

In order to verify the modeling of the transient simulation, in this section, a comparison of experimental and numerical results has been carried out.

3.4.1 Experimental setup

The experiment has been carried out in an experimental solar pond with cross-section area of 0.8×0.6 m^2 and depth of 1.0 m. The thicknesses of the LCZ, NCZ and UCZ are 0.4, 0.4 and 0.2 m, respectively. The salinity of LCZ is 20%; UCZ is 2%; NCZ is with the downward salinity increment of 2%/5cm. As shown in Fig.7, The solar pond was heated by a programmed temperature control system from LCZ, and the power system is controlled by a Programmable Logic Controller (PLC), and it controls the heating power based on the local solar radiation data and power update step is 1 minute. Solar radiation data is got by meteorological data of Jiaozuo City, Henan Province, China, and where the latitude is 35°20′. A 5 cm thickness cinders layer with porosity of 58% has been covered at bottom of LCZ. Temperature sensors with PTFE (Polytetrafluoroethylene) corrosion - resistant coating are set at the middle of solar pond along vertical direction. The model of the sensors is Pt-100 and accuracy is 0.01°C.

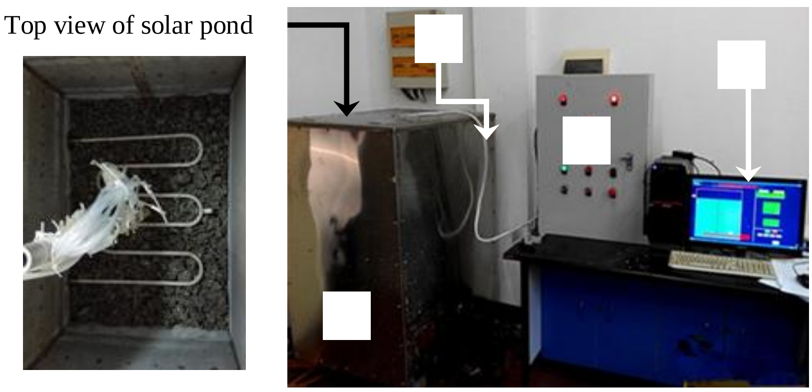

Fig.7 Laboratory solar pond system

The method to Determine the heating power p as following: if the time t is out of the range of sunshine time, then p=0; otherwise, p is calculated according to the solar radiation data and $\dot{q}(x)$. A voltage regulator has been used to stable the voltage, and the daily average error of the heating power has been controlled in the range of ±1.2W. The operation period is from 2 May to 9 May. Accordingly, for the numerical simulation, the temperature development is predicted by the modeling method presented in this study with the same date period.

3.4.2 Experimental results

Fig.8 gives experimental and numerical results comparison of temperature developments at different depth. It can be seen that the experimental temperature profiles show a larger increase and drop scope than numerical results, this is mainly caused by the different time step of experimental measurement and numercial study, which time step is 1 miniute for experiment and 1 hour for numerical simulation. The temperature increasing tends to slow during the last 2-3 days, this is caused by the change of weather which is related to a decrease of solar radiation. While the numerical temperature results shows a steady increasing trend, this is because that the numerical solar radiation is not affected by acctual weather changes.

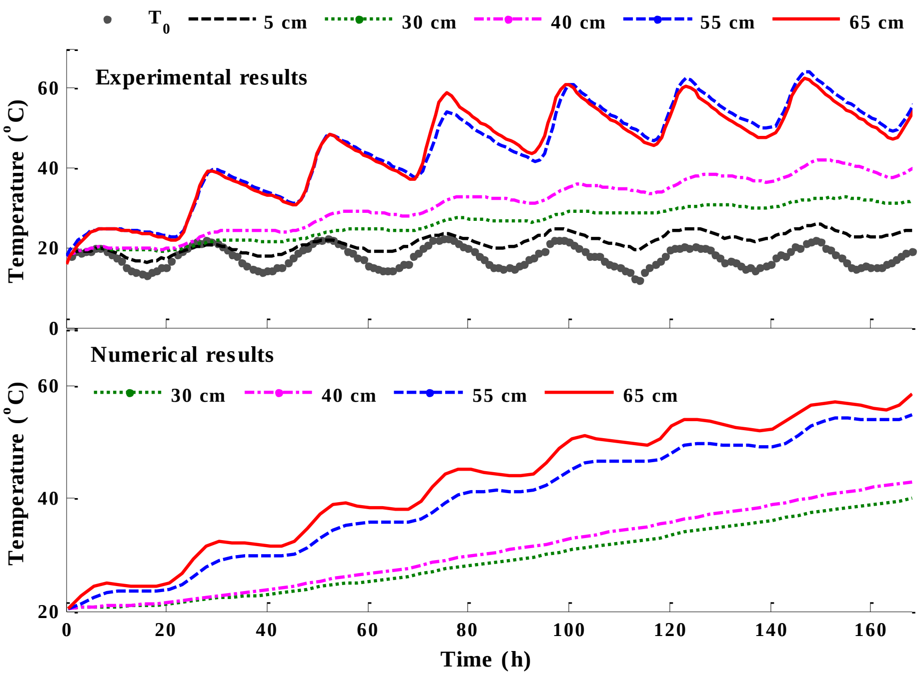

Fig. 8 Temperature developments at different depth for experimental and numerical results(T_0 is the ambient temperature)

Fig.9 gives the energy and exergy efficiency for both experimental and numerical results. It can be clearly seen that the numerical results are both higher than that of experiment. The difference of energy efficiency between numerical and experimental's is 1.41%; and the difference of exergy efficiency is 0.62%. However, the experimental and numerical results deviation of exergy efficiency is much bigger than energy efficiency. This distinction is caused by the difference of energy and exergy efficiencies, after all the energy efficiency only shows the quantity of energy, while exergy efficiency evaluates both quantity and quality.

In the numerical simulation, solar radiation is given according to the certain formulas, and for the experimental conditions, the actual transient solar radiation influences by many factors except for latitude and date, such as weather, air quality. However, solar pond is used for long term heat collection and storage, so it can be inferred for the long-term operation of the solar pond, the two results of experimntal and numerical should have the better consistency.

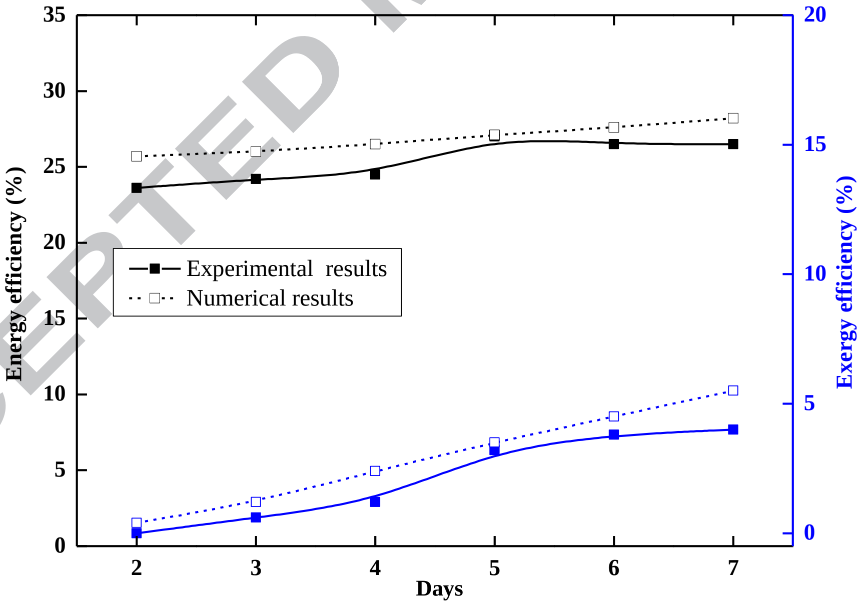

Fig. 9 Energy and exergy efficiency for experimental and numerical results

4. Conclusions

The exergy performance of solar pond porous media has been investigated based on temperature evolutions. Comparing with the exiting studies, this study has focused on the solar pond with porous media added in LCZ. The results show that:

- Adding most stone materials or cinders in LCZ could increase the solar pond temperature, and higher temperature is vital but not the only factor for the high energy/exergy efficiency, they are also depended on the volume heat capacity of the working medium.
- Among the four cases, adding cinders (case D) with low volume heat capacity, low conductivity and thermal diffusivity in LCZ gets the maximum energy and exergy efficiency of 32.62 % and 20.70 % respectively.
- The experimental study shows that the numerical energy and exergetic efficiency are both a little higher than experiment, and the same temperature difference leads to a bigger exergetic difference than energy.

Acknowledgements

This work has been carried out with the financial support of the Natural Science Foundation of China (NSFC) (U1404520).

References

[1] M. M. Zhang, P. Zhou, D. Q. Zhou. A real options model for renewable energy investment with application to solar photovoltaic power generation in China. Energy Economics 2016; 59: 213-226.

[2] Alcaraz, C. Valderrama, J.L. Cortina, A. Akbarzadeh, A. Farran. Enhancing the efficiency of solar pond heat extraction by using both lateral and bottom heat exchangers. Solar Energy 2016; 134: 82-94.

[3] Rubin, H., Bemporad, G.A., 1989. The advanced solar pond (ASP): basic theoretical aspects. Sol. Energy 43 (1), 35-44.

[4] Andrews, J., Akbarzadeh, A.. Enhancing the thermal efficiency of solar ponds by extracting heat from the gradient layer. Sol. Energy 2005; 78 (6), 704-716.

[5] Yaakob, Y., Date, A., Akbarzadeh, A., 2011. Heat extraction from gradient layer using. External heat exchangers to enhance the overall efficiency of solar ponds. In: IEEE First Conference on Clean Energy and Technology (CET) 2011.

[6] Leblanc, J., Akbarzadeh, A., Andrews, J., Lu, H., Golding, P.. Heat extraction methods from salinity-gradient solar ponds and introduction of a novel system of heat extraction for improved efficiency. Sol. Energy 2011; 85 (12), 3103-3142.

[7] Ismail Bozkurt, Mehmet Karakilcik. Exergy analysis of a solar pond integrated with solar collector. Solar Energy 2015; 112: 282-289.

[8] A.A. Abdullah , K.A. Lindsay, A.F. AbdelGawad. Construction of sustainable heat extraction system and a new scheme of temperature measurement in an experimental solar pond for performance enhancement. Solar Energy 2016; 130: 10-24.

[9] G.D. Zhang, Z.Y. Wu, F.Q.Cheng, Z. Min, Duu-Jong Lee. Thermophilic digestion of waste-activated sludge coupled with solar pond. Renewable Energy 2016; 98: 142-147.

[10] Mustafa Erden, Mehmet Karakilcik, Ibrahim Dincer. Performance investigation of hydrogen production by the flat-plate collectors assisted by a solar pond. International journal of hydrogen energy 2017; 42(4): 2522-2529.

[11] Francisco Suárez, Jeffrey A. Ruskowitz , Scott W. Tyler , Amy E. Childress. Renewable water: Direct contact membrane distillation coupled with solar ponds. Applied Energy 2015; 158: 532-539.

[12] J.J. Yu, M.P. Zheng, Q. Wu, Z. Nie, L.Z. Bu. Extracting lithium from Tibetan Dangxiong

Tso Salt Lake of carbonate type by using geothermal salinity-gradient solar pond. Solar Energy 2015; 115: 133-144.

[13] Sura Tundee, Narong Srihajong, Suparerk Charmongkolpradit. Electric power generation from solar pond using combination of thermosyphon and thermoelectric modules. Energy Procedia 2014; 48: 453 -463.

[14] A.Date , A. Akbarzadeh. Theoretical study of a new thermodynamic power cycle for thermal water pumping application and its prospects when coupled to a solar pond. Applied Thermal Engineering 2013; 58: 511-521.

[15] R. Singh, S. Tundee, A. Akbarzadeh. Electric power generation from solar pond using combined thermosiphon and thermoelectric modules. Solar Energy 2011; 85: 371-378.

[16] Hitesh Bindra, Pablo Bueno, Jeffrey F. Morris, Reuel Shinnar. Thermal analysis and exergy evaluation of packed bed thermal storage systems. Applied Thermal Engineering 2013; 52: 255-263.

[17] D.D. Weeks, H.C. Bryant What happens when a solar pond boils Proc. Annual Meeting-Am. Sect. Int. Sol. Energy Soc. 1981; USA, 4(CONF-810509-vol. 1).

[18] F. Al-Juwayhel, M.M. El-Refaee. Thermal performance of a combined packed bed-solar pond system-a numerical study. Applied Thermal Engineering 1998; 18: 1207-23.

[19] H. Wang, J.N. Zou, J.L. Cortina, J. Kizito. Experimental and theoretical study on temperature distribution of adding coal cinders to bottom of salt gradient solar pond. Solar Energy 2014; 110: 756-767.

[20] H. Wang, X. Yu, F. Shen, L. Zhang. A laboratory experimental study on effect of porous medium on salt diffusion of salt gradient solar pond. Solar Energy 2015;122:630-9.

[21] A.A. Hill, M.Carr. Stabilising solar ponds by utilising porous materials. Adv Water Resour 2013; 60:1-6.

[22] Choubani Karim, Zitouni Slim, Charfi Kais, Safi Mohamed Jomâa, Aliakbar Akbarzadeh. Experimental study of the salt gradient solar pond stability. Solar Energy 2010; 84(1): 24-31.

[23] Choubani Karim, Zitouni Slim, Charfi Kais, Safi Mohamed Jomâa, Aliakbar Akbarzadeh. A laboratory experimental study of mixing the solar pond gradient zone. Solar Energy 2011; 85(2): 404-417.

[24] G. Kalaiarasi, R. Velraj, Muthusamy V. Swami. Experimental energy and exergy analysis of a flat plate solar air heater with a new design of integrated sensible heat storage. Energy 2016; 111: 609-619.

[25] A. Bejan, Two thermodynamic optima in the design of sensible heat units for energy storage. ASME J. Heat Transfer 1978; 100: 708–712.

[26] Ali A. Dehghan, Alireza Movahedi, Mohsen Mazidi. Experimental investigation of energy and exergy performance of square and circular solar ponds. Solar Energy 2013; 97: 273-284.

[27] Ayhan Atiz, Ismail Bozkurt, Mehmet Karakilcik, Ibrahim Dincer. Investigation of turbidity effect on exergetic performance of solar ponds. Energy Conversion and Management 2014; 87: 351-358.

[28] Mehmet Karakilcik, Ibrahim Dincer. Exergetic performance analysis of a solar pond. International Journal of Thermal Sciences 2008; 47: 93-102.

[29] Morteza Khalilian. Experimental and numerical investigations of the thermal behavior of

small solar ponds with wall shading effect. Solar Energy 2018, 159(1): 55-65.

[30] A.K. Saxena, S. Sugandhi, M. Husain. Significant depth of ground water table for thermal performance of salt gradient solar pond. Renewable Energy 2009; 34:790-793.

[31] R.B. Mansour et al., C. T. Nguyen, N. Galanis. Transient heat and mass transfer and long-term stability of a salt-gradient solar pond. Mechanics Research Communications 2006; 33(2): 233-249.

[32] Giestas, M., Pina, H., Joyce, A., The influence of radiation absorption on solar pond stability. Int. J. Heat Mass Transfer 1996; 39 (18), 3873-3885.

[33] Zhang H.F., Solar Energy Thermal Application and Simulation, (Eds.: Y.C. Zhang), Xi'an Jiao Tong University Press Co., LTD., 2012, pp. 23-33.

[34] D.W. Kaufmann. Sodium chloride the production and properties of salt and brine. Chemical Reactions 1960. Reinhold Publishing Corp, New York.

[35] M.R. Jaefarzadeh. Thermal behavior of a small salinity-gradient solar pond with wall shading effect. Solar Energy 2004; 77(3):281-290.

[36] R. Petela. Exergy of undiluted thermal radiation. Solar Energy 2003; 74(6): 469-488.

Highlights

- Exergetic performance of solar pond with porous media is investigated.
- Transient exergy distribution has been numerical and experimental studied.
- The effect of porous media properties on exergy performance is discussed.